XPS characterisation of core–shell silica–polymer composite particles synthesised by atom transfer radical polymerisation in aqueous media

C. Perruchot [a], M.A. Khan [a], A. Kamitsi [a], S.P. Armes [a,*], J.F. Watts [b], T. von Werne [c], T.E. Patten [c]

[a] *Department of Chemistry, School of Life Sciences, University of Sussex, Falmer, Brighton, East Sussex BN1 9QJ, UK*
[b] *The Surface Analysis Laboratory, School of Engineering, University of Surrey, Guildford, Surrey GU2 7XH, UK*
[c] *Department of Chemistry, University of California at Davis, One Shields Avenue, Davis, CA 95616-5295, USA*

Abstract

Near-monodisperse, siloxane-functionalised silica particles are used as a colloidal substrate for the surface-initiated polymerisation of various hydrophilic methacrylates: oligo(ethylene glycol) methacrylate (OEGMA), 2-(*N*-morpholino)ethyl methacrylate (MEMA), and ammonium 2-sulfatoethyl methacrylate (SEM) by atom transfer radical polymerisation in aqueous media at room temperature. The bulk and surface compositions of the resulting composite particles were assessed using various techniques. Thermogravimetric analysis of the resulting silica–polymer composites indicated polymer loadings of 5.4–8.6%, depending on the nature, structure and target degree of polymerisation (D_p). Dynamic light scattering studies indicate increases in hydrodynamic diameter of 14–87 nm compared to the reference silica particles. FT-IR spectroscopy confirmed additional features characteristic of the carbonyl group and pendant end-chain functionalities of the methacrylic polymer chains. The elemental and chemical surface compositions of the initial silica particles and final polymer-grafted composite particles were extensively investigated by X-ray photoelectron spectroscopy (XPS). The composite particles had appreciably higher C/Si atomic ratios, compared to the original initiator-functionalised silica particles, and these ratios increased with increasing target D_p. In addition, close inspection revealed that the relative intensities of the various components of the peak-fitted C1s envelopes varied significantly, depending on the target degree of polymerisation and the chemical structure of the methacrylic monomer. Moreover, in the case of the MEMA and SEM polymerisations, new nitrogen (MEMA) and sulfur (SEM) XPS signals were detected. This XPS study confirmed the presence of a thin outer layer of grafted polymer chains surrounding the silica particles.
© 2004 Elsevier Ltd. All rights reserved.

Keywords: Composite particles; Silica sol; Surface-initiated polymerisation; X-ray photoelectron spectroscopy; Atom transfer radical polymerisation; Hydrophilic functionalised methacrylate monomers

1. Introduction

The synthesis of polymers with well-defined compositions, architectures and functionalities continues to be of considerable interest. The pioneering work of Matyjaszewski and co-workers and Sawamoto's group in 1995 led to the development of atom transfer radical polymerisation (ATRP) [1]. This chemistry is very tolerant of monomer functionality, allows the synthesis of polymers of various architectures (statistical copolymers, block copolymers star polymers, etc.), with good control over the target molecular weight and molecular

---

* Corresponding author.
E-mail address: S.P.Armes@sussex.ac.uk (S.P. Armes).

weight distribution (polydispersities are typically less than 1.2–1.3). Matyjaszewski and Xia have recently reviewed atom transfer radical polymerisation (ATRP) and described the various monomers, initiators and ligands combinations that are required for optimal results [2]. Our group has recently reported the ATRP, usually in protic media, of various non-ionic, betaine and polyelectrolytic monomers [3–12]. Rapid rates of polymerisation and very high conversions of a wide range of hydrophilic (meth)acrylate monomers have been obtained at room temperature. ATRP also allows the synthesis of new stimulus-responsive diblock copolymers that undergo micellisation in aqueous solution on adjusting the solution pH or temperature.

In recent years there has been increasing interest in surface-initiated ATRP from planar and colloidal substrates, with both latexes and inorganic particles being examined [13,14]. For example, Jones and Huck reported the surface-initiated ATRP of various methacrylic monomers from a thiol-functionalised planar gold surface [15]. The polymer thickness and morphology were characterised by ellipsometry and atomic force microscopy (AFM). This study suggested that the polymerisation was controlled, as a linear increase in thickness with time was obtained. Dense polymeric brushes with thicknesses of up to 125 nm were produced. AFM indicated that a uniform, continuous and smooth coating of polymer chains covered the gold substrate. The chemically grafted polymer chains changed the surface properties of the planar substrate, as demonstrated by contact angle measurements. The living character of ATRP was examined by the block copolymerisation of MMA with HEMA by sequential monomer addition. A significant increase in the polymer thickness was observed, suggesting that MMA-b-HEMA diblock copolymer brushes were obtained. Similarly, Shah et al. reported the modification of a planar gold surface using ATRP initiator-functionalised thiols and demonstrated the subsequent polymerisation of various methacrylates using this substrate [16]. Fukuda and co-workers modified planar glass substrates with a chloro-functionalised silane, and subsequently grafted a sugar-based methacrylate using ATRP [17]. Brittain and co-workers prepared styrene-MMA and styrene-methyl acrylate diblock copolymers by surface-initiated ATRP from planar silica substrates. The surface morphology of the resulting brushes was extensively characterised by atomic force microscopy (AFM) [18,19]. Matyjaszewski et al. reported the modification of silicon wafers using a bromo-functionalised siloxane, followed by surface-initiated ATRP of styrene and various acrylate monomers [20]. Again, a linear increase in the polymer brush thickness was observed with reaction time.

Of particular relevant to the present work, Charleux and co-workers reported the surface-initiated aqueous ATRP of both 2-(methacryloyloxy)ethyl trimethylammonium chloride and 2-hydroxyethyl acrylate using initiator-functionalised latex particles [21]. Hallensleben and co-workers grafted bromo-functionalised thiols onto gold nanoparticles, and used this modified inorganic substrate for the ATRP of n-butyl acrylate [22]. The same group also reported the surface modification of silica particles by chloro-functionalised silanes and the subsequent polymerisation of styrene by ATRP. Thermogravimetric analysis confirmed increasing amounts of grafted polymer chains with increasing surface concentration of initiator and FT-IR spectroscopy indicated characteristic bands due to the grafted polystyrene [23]. Mandal et al. reported the preparation of hollow polymer microspheres by the polymerisation of benzyl methacrylate from surface-initiated silica particles, with subsequent removal of the silica cores by chemical etching with HF [24]. Von Werne and Patten reported the surface modification of silica particles by bromo-functionalised siloxanes with subsequent polymerisation of styrene and methacrylate monomers by ATRP in organic solvent [25,26]. More recently, the same group reported the preparation of core–shell CdS-silica nanoparticles Subsequent surface modification with a bromo-functionalised siloxane allowed polymer chains to be grafted with controlled thicknesses [27]. The resulting hybrid particles retained the photoluminescence properties of the CdS precursor after solvent casting onto planar substrates. Surface-initiated ATRP is thus an effective 'grafting from' method for various (meth)acrylate monomers and styrene. Recently, Chen et al. reported the polymerisation of various anionic and cationic methacrylate monomers onto surface-functionalised silica particles by surface-initiated ATRP in protic media [28]. The resulting dense polyelectrolyte grafted-silica particles were extensively characterised using dynamic light scattering, zeta potential, thermogravimetric analysis, scanning electron microscopy and diffuse reflectance infrared Fourier transfer spectroscopy (DRIFTS). This study clearly showed that the colloidal stabilities of the resulting composite particles were governed by the grafted polymer chains. Chen and Armes also reported the use of a tailor-made cationic macro-initiator for the facile surface modification of ultrafine anionic sols by electrostatic adsorption prior to surface ATRP [29].

Recently we reported the use of surface-functionalised 300 nm silica particles for the polymerisation of various hydrophilic methacrylates by aqueous ATRP [30]. The physicochemical properties of the resulting polymer-grafted particles were characterised by thermogravimetric analysis, dynamic light scattering, scanning electron microscopy and preliminary X-ray photoelectron spectroscopy (XPS) results. This study indicated that the resulting inorganic–organic hybrid particles had core–shell morphologies, as expected. It was also shown that the grafted polymer chains influ-
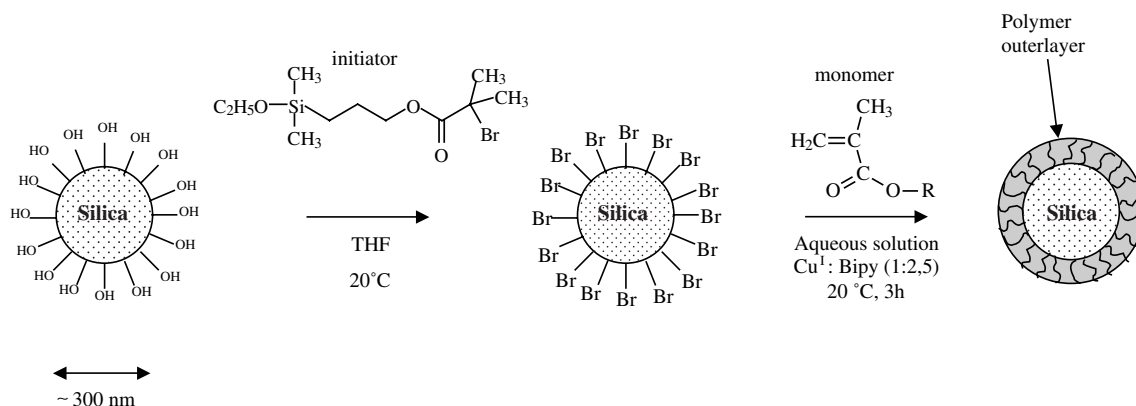
Fig. 1. Schematic representation of the functionalised siloxane-based ATRP initiator and subsequent synthesis of the polymer-grafted silica particles by ATRP.

enced the colloidal stability of the silica particles. Herein we describe a more detailed XPS study of the surface compositions of selected silica–polymer composite particles. A schematic representation of the surface modification of the initiator-functionalised silica particles and subsequent polymerisation of hydrophilic methacrylates via aqueous ATRP is presented in Fig. 1.

2. Experimental

2.1. Synthesis of the colloid silica sol

The colloidal silica particles were prepared according to the Stöber method [31]. A full description of the synthesis protocol has been previously reported [25]. The weight-average particle diameter was determined by disk centrifuge photosedimentometry and scanning electron microscopy to be around 300 nm.

2.2. Synthesis of the initiator-grafted silica particles

(3-(2-Bromoisobutyryl)propyl)dimethylethoxy silane (see Table 1) was grafted onto the silica surface and acted as the ATRP initiator. Von Werne and Patten have already reported a detailed description of the synthesis, characterisation and grafting protocol for this initiator [25]. Elemental analyses indicated that the initiator-grafted silica particles contained 0.40% bromine, which corresponded to an average of 0.50 mmol initiator per gram of silica particles. After purification and drying, the surface-functionalised silica particles were then used as a finely divided colloidal substrate for the synthesis of various hydrophilic functionalised methacrylates by aqueous ATRP.
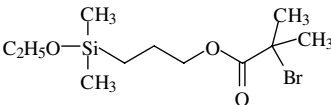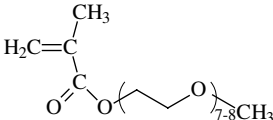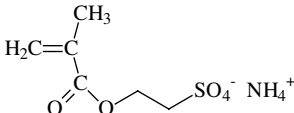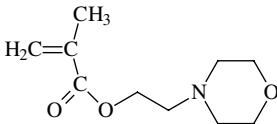
2.3. Synthesis of the polymer-grafted silica particles

The three hydrophilic methacrylates examined in this study were monomethoxy-capped oligo(ethylene glycol) methacrylate [OEGMA], ammonium 2-sulfatoethyl methacrylate [SEM, supplied as a 25% aqueous solution] and 2-(N-morpholino)ethyl methacrylate [MEMA]. Table 1 reports the monomers structure. OEGMA and SEM were both donated by Cognis Performance Chemicals (Hythe, UK) and MEMA was purchased from Polysciences Inc. (USA). The chemical structures of these monomers, which were used without further purification, are shown in Table 1. Copper(I) chloride, copper(I) bromide and 2,2′-bipyridine [bpy] were employed as the catalyst and ligand species for the ATRP syntheses. Doubly-distilled de-ionised water was used to prepare aqueous dispersions of the silica particles.

In a typical synthesis protocol, the silica particles (300 mg) were dispersed in water (3.0 ml) and the Cu(I)X and bpy (X = Cl or Br; molar ratio of bpy/Cu = 2.5) were dissolved into the hydrophilic methacrylate monomer. On mixing these two degassed solutions at 20 °C under a nitrogen atmosphere, an exotherm of a few degrees was immediately observed and the dark brown solution became progressively more viscous, indicating the onset of polymerisation. After stirring for approximately 3 h at ambient temperature, the polymerisation was terminated by exposure to air. This caused the solution to turn blue, indicating aerial oxidation of Cu(I) to Cu(II). Separation of the polymer-grafted silica particles from the aqueous solution was achieved by centrifugation (3000 rpm for 10 min). The supernatant was discarded and the sedimented particles were redispersed in de-ionised doubly-distilled water with the aid of an ultrasonic bath. After several centrifugation–redispersion cycles, the isolated particles were off-white in colour, indicating low levels of residual

Table 1

Chemical structures of the functionalised siloxane initiator and hydrophilic methacrylic monomers used in this work

Name	Chemical structure
(3-(2-bromoisobutyryl)propyl) dimethylethoxysiloxane	
Oligo(ethylene glycol) methacrylate [OEGMA]	
Ammonium 2-sulfatoethyl methacrylate [SEM]	
2-(*N*-Morpholino)ethyl methacrylate [MEMA]	

ATRP catalyst. The resulting purified silica–polymer composite particles were then vacuum-dried overnight prior to analysis. The sample notation is as follows: silica-I-monomer name(X), where X represents the target degree of polymerisation as calculated from the monomer/surface initiator molar ratio. In this study, relatively high degrees of polymerisation were targeted compared to conventional ATRP because thick polymer brushes were desired. Table 2 summarises the target degrees of polymerisation, the catalyst species and catalyst/initiator molar ratios used in the ATRP synthesis of the core–shell silica–polymer composite particles.

2.4. Thermogravimetric analysis (TGA)

Thermogravimetric analyses were carried out using a Perkin Elmer TGA-7 instrument. The sample (20–30 mg; analysed after overnight drying in a vacuum dessicator) was heated from room temperature up to 800 °C in air at a scan rate of 20 °C min^{-1} to ensure complete combustion of all organic species. The residue is assumed to be non-combustible silica. The observed mass loss was attributed to the quantitative pyrolysis of the polymer component. In the case of the polymer-silica composite particles, the total weight loss was corrected using the weight loss determined for the initiator-functionalised silica particles.

2.5. Helium pycnometry

The densities of the dried particles were determined by helium pycnometry using a Micromeritics AccuPyc 1330 instrument. Samples were analysed after overnight drying in a vacuum dessicator to remove moisture.

Table 2

Target degrees of polymerisation, catalyst species and catalyst/initiator ratios used for the synthesis of the polymer-grafted silica particles

Sample description	Target D_p	Catalyst	Catalyst/initiator ratio
SiO$_2$-init-OEGMA	250	CuCl	20
SiO$_2$-init-OEGMA	500	CuCl	20
SiO$_2$-init-OEGMA	1000	CuCl	20
SiO$_2$-init-MEMA	500	CuBr	10
SiO$_2$-init-SEM	500	CuBr	10

2.6. Dynamic light scattering studies

The hydrodynamic diameters of a highly dilute aqueous suspension of either silica or silica–polymer composite particles were determined by dynamic light scattering (DLS). DLS measurements were performed using a Malvern 4700 instrument. This instrument was equipped with a 75 mW argon ion laser. The scattered light intensity was measured at a scattering angle of 90°. All measurements were carried out at 25 °C. The particles were assumed to be near-monodisperse, non-interacting spheres and the Stokes–Einstein equation was used to determine the hydrodynamic diameters.

2.7. FT-IR spectroscopy

FT-IR spectra were obtained using a Perkin Elmer FTIR Spectrum One instrument. The average number of scans per spectrum was 256 and the spectral resolution was 4 cm^{-1}.

2.8. Surface analysis by X-ray photoelectron spectroscopy (XPS)

XPS analyses were performed using a Thermo VG Scientific Sigma Probe spectrometer. A twin MgKα X-ray source ($E = 1253.6$ eV) was used with a 500 μm diameter spot size. The pass energy was set at 100 eV for the survey spectra and at 20 eV for the high resolution spectra of all elements of interest. High resolution C1s, O1s and Si2p spectra were recorded for all three monomers, with N1s and S2p spectra also being recorded for the ammonium 2-sulfatoethyl methacrylate (SEM) and 2-(N-morpholinoethyl) methacrylate (MEMA). Data processing was performed using the supplier's software (PC-based Avantage 1.46 software). Quantitative surface compositions (in atom %) were calculated for each specimen using the peak areas of the high resolution core spectra of the elements present, after Shirley baseline subtraction and using Schofield sensitivity factors corrected for instrumentation transmission function. The peak fitting parameters were the binding energy measured at the peak maxima, the full width at half maximum of the peak (FWHM), the total area of the peak after baseline subtraction and the Gaussian-to-Lorentzian ratio (G/L ratio). All peak fits were obtained within the constraints of chemical intuition. The quality of each peak fit was obtained by determining the χ^2, which is the sum of the squares of the difference between the experimental signal and the fitted envelope, at 0.1 eV intervals over the spectral region of interest. In all cases the binding energies of the various components of the peak-fitted signals were determined by setting the reference C–C/C–H component at 285.0 eV, to correct for sample charging effects. When preparing the samples, a piece of aluminium foil (0.8×0.8 cm) was covered with double-sided tape. The powdered specimen was applied onto the tape in order to mask the entire surface, and any excess was removed to avoid contamination of the XPS spectrometer.

3. Results and discussion

The results reported in this work concern both the bulk and surface compositions of the polymer-grafted silica particles, the initiator-functionalised silica and the silica precursor particles. Thermogravimetric analyses, density measurements and FT-IR spectra provide information regarding the bulk compositions, whereas XPS is sensitive to the surface compositions. One aim of this work was to demonstrate that surface-initiated ATRP is a particularly effective method for the covalent grafting of various hydrophilic methacrylates onto near-monodisperse silica particles in aqueous media. Since relatively high degrees of polymerisation were targeted, somewhat higher catalyst/initiator ratios were used compared to conventional ATRP syntheses in order to improve control over the polymerisation (see Table 2).

The polymer mass loading was assessed by thermogravimetric analysis of the composite particles, with the initiator-functionalised silica particles acting as reference materials. Table 3 reports the polymer contents obtained for various methacrylates, depending on the degree of polymerisation targeted. In the case of the polymer-grafted silica particles, the total weight loss was corrected by taking into account the weight loss observed for the initiator-functionalised silica particles due to pyrolysis of the organic initiator and removal of surface moisture. For a fixed target D_p of 500, the corrected polymer contents obtained for the homopolymerisation of OEGMA, SEM and MEMA ranged from 5.3 to 8.6 wt. %, with the highest loading being obtained for MEMA homopolymer (see Table 3). MEMA is relatively well behaved under aqueous ATRP conditions so this probably reflects a higher conversion for this monomer [11]. Moreover, increasing the target degree of polymerisation from 250 to 1,000 for the OEGMA syntheses leads to higher polymer contents and also lower composite densities, as expected.

In similar manner, the density measurements clearly demonstrate a slight decrease of the composite particles density compared to reference surface-functionalised silica particles (see Table 3), depending on the nature of the monomer and targeted degree of polymerisation. The decrease of the composite density is in good agreement with the increase of the polymer content as previously observed by TGA.

Dynamic light scattering studies were carried out on the polymer-grafted silica particles and also on the initiator-functionalised silica particles. In all case, the

Table 3
Summary of the polymer contents determined by thermogravimetry, particle densities obtained from helium pycnometry, average hydrodynamic particle diameters measured by dynamic light scattering and adsorbed amounts (Γ) for the initiator-functionalised silica particles and the polymer-grafted silica particles

Sample description	Polymer content (%)	Particle densities (g cm^{-3})	Particle diameter (nm)	Γ (mg m^{-2})
SiO$_2$-init	–	1.90[a]	360[a]	
		2.02[b]	320[b]	
SiO$_2$-init-OEGMA(250)	5.4	1.86[a]	370[a]	6.4
SiO$_2$-init-OEGMA(500)	6.5	1.82[a]	400[a]	7.8
SiO$_2$-init-OEGMA(1000)	8.2	1.75[a]	440[a]	10.0
SiO$_2$-init-MEMA(500)	8.6	1.90[b]	400[b]	10.1
SiO$_2$-init-SEM(500)	5.3	1.97[b]	560[b]	6.0

[a] Silica particles of 356 nm were used for this set of experiments.
[b] Silica particles of 318 nm were used for this set of experiments.

intensity-average hydrodynamic diameters of the composite particles are larger than that measured for the uncoated silica sol (see Table 3). Moreover, an increase in the hydrodynamic thickness due to the grafted polymer chains is observed as the target degree of polymerisation is increased. This observation is in good agreement with the TGA and density measurements, as previously discussed.

If we assume that the initiator-functionalised silica sol comprises non-porous, spherical particles with a mean diameter (D) of 340 nm, and particle density ρ, one can estimate the specific surface area, A_s, of the silica sol using the relationship $A_s = 6/(\rho \cdot D)$. The calculated A_s values are close to 10 m^2 g^{-1}. Combining these values with the TGA data, the polymer loadings correspond to quite high Γ values, ranging from 3.7 up to 10.1 mg m^{-2}. These high Γ values suggest that relatively dense polymer brushes are grafted onto the silica surface.

Confirmation of the presence of the grafted polymer on the silica particles can be obtained by FT-IR spectroscopy. Fig. 2 shows the FT-IR spectra, recorded in the 550–1800 cm^{-1} range, for initiator-functionalised silica particles, OEGMA homopolymer and OEGMA-grafted silica particles with target degrees of polymerisation of 250 and 500, respectively. For the polymer-grafted silica particles, Characteristic bands are clearly detected at 1257, 1349, 1460 and 1714 cm^{-1}. These bands are assigned to C–O stretching, CH/CH$_2$ scissor and to C=O stretching, respectively [32] and are characteristic of the grafted methacrylic polymer (in this case OEGMA homopolymer). Similar bands were also detected in the case of SEM- and MEMA-grafted silica particles (spectra not shown). Moreover, increasing the target degree of polymerisation led to a significant increase in the intensities of these bands relative to the silica bands. This observation demonstrates, albeit qualitatively, that the polymer loadings increase with increasing target degrees of polymerisation. This is in good agreement with the results obtained from the TGA and density measure-
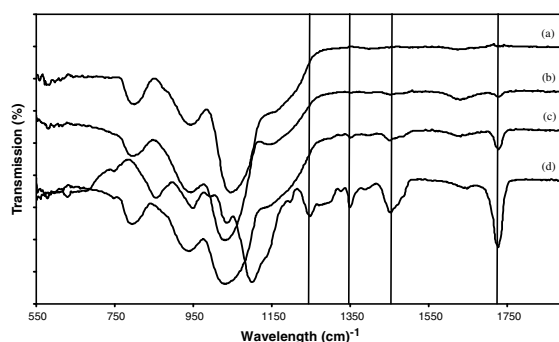

Fig. 2. FT-IR spectra recorded for: (a) the initiator-functionalised silica particles, (b) silica-init-OEGMA(250), (c) silica-init-OEGMA(500), and (d) OEGMA homopolymer reference, respectively.

ments, and thus confirms the presence of the grafted polymer chains at the silica surface.

Fig. 3 shows the XPS survey spectra for bare silica (Fig. 3a), initiator-functionalised silica (Fig. 3b) and three polymer-grafted silica sols, namely silica-I-OEGMA(500) (Fig. 3c), silica-I-MEMA(500) (Fig. 3d) and silica-I-SEM(500) (Fig. 3e).

For the bare silica particles, the characteristic signals for silicon (Si2p at 103 eV and Si2s at 155 eV) and oxygen (O1s at 533 eV and oxygen Auger Okll at 740 eV) are clearly detected. An additional weak carbon signal (C1s at 285 eV) is also detected. This latter feature probably indicates incomplete hydrolysis of the alkoxide precursor used for the synthesis of the silica particles.

For the initiator-functionalised silica particles (Fig. 3b), the characteristic signals due to silicon, oxygen and carbon are again detected. However, the carbon signal is noticeably stronger compared to bare silica; this due to the additional carbon atoms in the bromosiloxane-based initiator.

Turning to the polymer-grafted silica particles, the characteristic silicon and oxygen signals from the silica
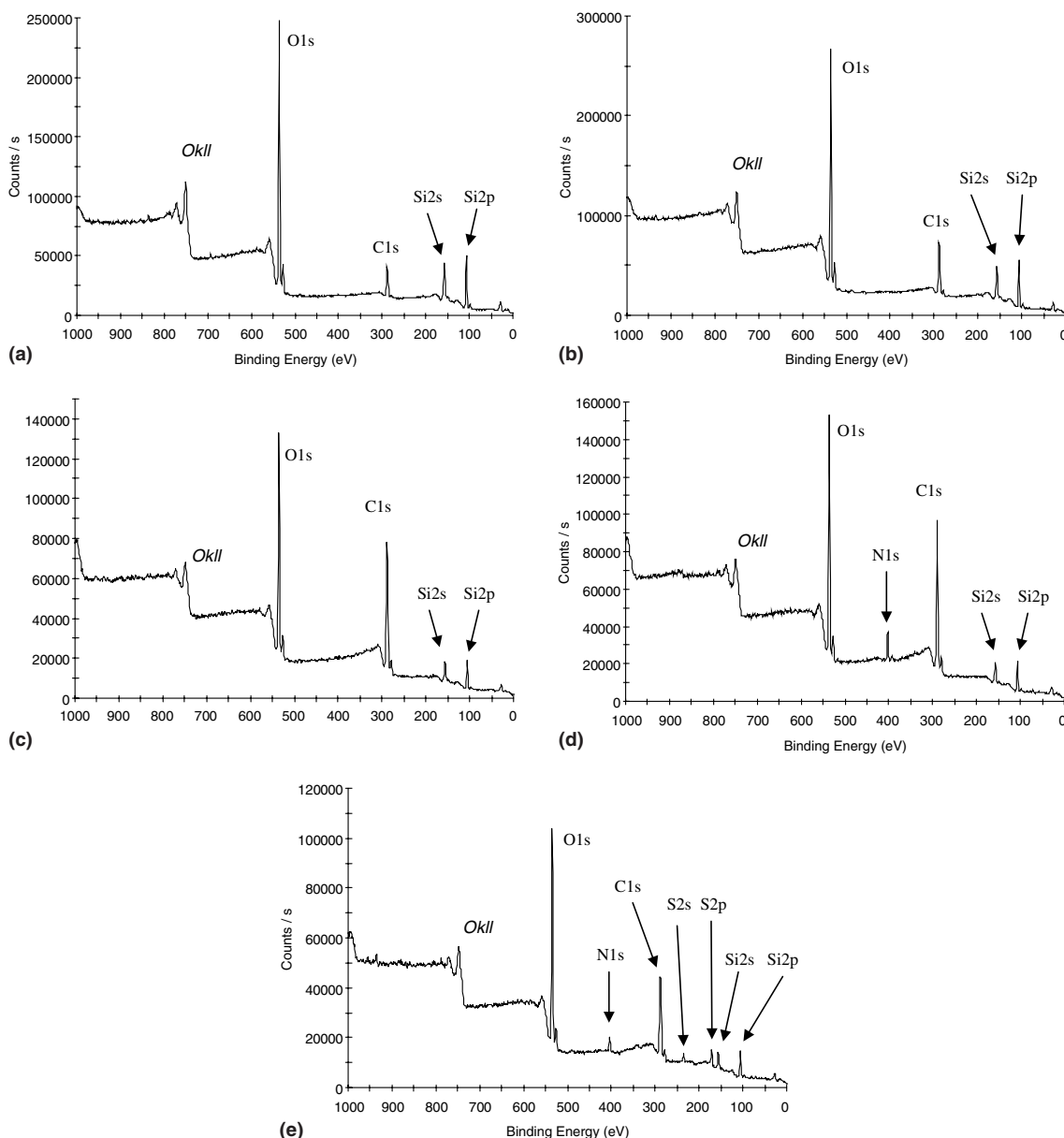
Fig. 3. XPS survey spectra of: (a) the bare silica sol, (b) the initiator-functionalised silica particles, (c) silica-init-OEGMA(500), (d) silica-init-MEMA(500), and (e) silica-init-SEM(500) particles, respectively.

substrate are still observed, but with lower intensity, together with more intense carbon C1s signals (see Fig. 3c–e respectively), compared to the initiator-functionalised silica particles (Fig. 3b). Moreover, in case of silica-I-MEMA(500) (Fig. 3d) and silica-I-SEM(500) (Fig. 3e) composites, additional weak signals assigned to nitrogen N1s at 400 eV are also detected, as well as sulfur S2p and S2s signals (at 169 and 230 eV, respectively) for the silica-I-SEM(500) composite. These elements are characteristic of the grafted polymer chains (see chemical structures in Table 1) but not the inorganic substrate, therefore they can be used as unambiguous elemental markers. For the three polymer-silica composite particles, the silica sol, the siloxane initiator and the grafted polymer chains all contribute to the overall C1s signal. Using the initiator-functionalised silica as a reference materials, inspection of the survey spectra for the three composites confirms that polymerisation of the hydrophilic methacrylic monomers always leads to a significant increase in the C1s signal intensity relative to the

Si2p signal. Given that the XPS sampling depth is typically less than 10 nm, this increase, in addition to the detection of specific elemental markers (i.e. nitrogen and/or sulfur), is a clear indication of the presence of an outer layer of grafted polymer chains masking the underlying silica surface.

Peak fitting of the high resolution spectra obtained for selected elements was performed so as to provide oxidation state information and hence determine which chemical species were present at the outermost surface of the reference silica and composite particles [33–35]. Fig. 4 displays the peak-fitted C1s signals for the bare silica

sol (see Fig. 4a), the initiator-functionalised silica (Fig. 4b), silica-I-OEGMA(500) (Fig. 4c), silica-I-SEM(500) (Fig. 4d) and silica-I-MEMA(500) (Fig. 4e), respectively.

For the bare silica sol, the C1s signal can be peak-fitted with three components. The main component, centred at 285.0 eV, is assigned to CC/CH carbon species. The second and third components, centred at 286.80 and 288.69 eV, are attributed to C–O and O–C=O species, respectively. These latter species are probably due to incomplete hydrolysis of the alkoxide precursor during the Stöber synthesis of the silica particles [31].
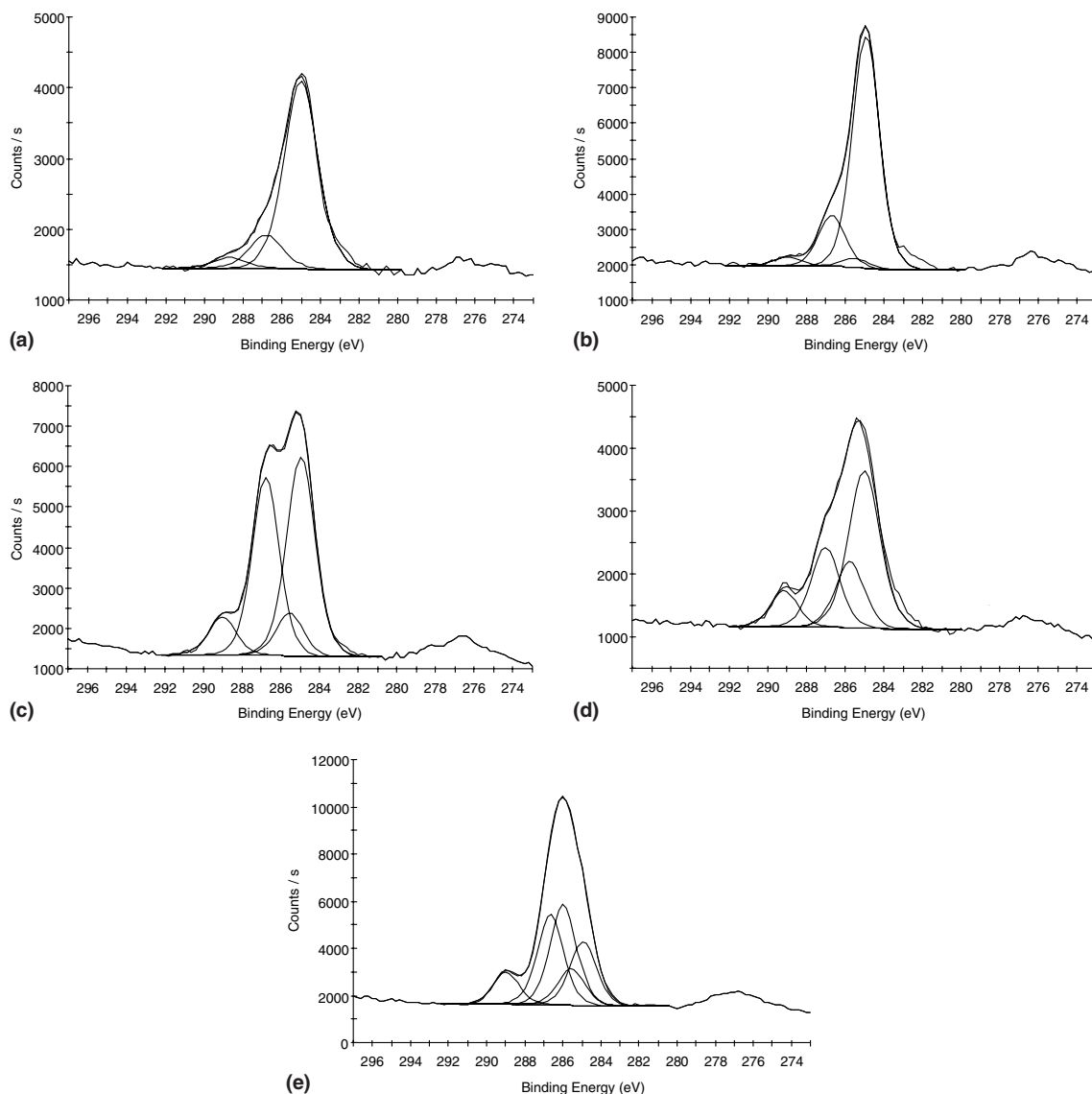

Fig. 4. Peak-fitted C1s signals of: (a) the bare silica sol, (b) the initiator-functionalised silica particles, (c) silica-init-OEGMA(500), (d) silica-init-SEM(500), and (e) silica-init-MEMA(500) particles, respectively.

For the initiator-functionalised silica particles, satisfactory peak fitting of the C1s signal required four components, which are assigned to (i) aliphatic carbon atoms (main component centred at 285.0 eV), (ii) carbon atoms that are adjacent to carbonyl groups (i.e. C–COO species centred at 285.62 eV) and carbon atoms that either (iii) form single bonds with oxygen (i.e. C–O centred at 286.76 eV) or (iv) form double bonds with oxygen (i.e. O–C=O centred at 289.06 eV), respectively.

In the case of silica-I-OEGMA(500) composite particles (Fig. 4c), the C1s signal was peak fitted with four components, which are assigned to aliphatic carbon atoms (centred at 285.0 eV), carbon atoms in β-position of carbonyl groups (i.e. C–COO, centred at 285.59 eV), carbon atoms linked to oxygen species of the characteristic methacrylate functionality groups (i.e. C–O and O–C=O centred at 286.81 eV and 289.06 eV, respectively). Depending on the initial target degree of polymerisation, similar values of the binding energies are determined. However, variation of the relative intensities of each component is observed for the various components of the peak-fitted C1s signal (see Table 4). This result demonstrates that the binding energies of the carbon components are independent of the initial degree of polymerisation of the OEGMA monomer, as expected, and the observed changes in the relative intensities are consistent with the increasing target degrees of polymerisation. These observations are discussed further below.

For the silica-I-SEM(500) composite (Fig. 4d), the C1s signal was peak-fitted with four components assigned to (i) aliphatic carbon, (ii) carbon atoms adjacent to carbonyl groups and/or carbon species linked to sulfur atoms (i.e. C–COO and/or C–S species centred at 285.75 eV), (iii) carbon atoms that form single bonds with oxygen (i.e. C–O centred at 287.00 eV) and (iv) carbon atoms that form double bonds with oxygen (i.e. O–C=O centred at 289.15 eV), respectively.

For the silica-I-MEMA(500) composite (see Fig. 4e), satisfactory peak-fitting of the carbon signal required five components. These components are assigned to (i) aliphatic carbon, (ii) carbon adjacent to carbonyl groups (285.61 eV), (iii) carbon atoms bonded to nitrogen (i.e. C–N centred at 286.03 eV), (iv) carbon atoms that form single bonds with oxygen (i.e. C–O centred at 286.70 eV) and (v) carbon atoms that form double bonds with oxygen (i.e. O–C=O centred at 289.04 eV), respectively.

The binding energies determined for the various components of the peak-fitted C1s signals are in good agreement with the respective carbon functionalities in the bromosiloxane initiator and in the respective methacrylate repeat units [34,35].

The relative intensities of the various components of the peak-fitted C1s signals obtained for the various silica–polymer composites do not match the theoretical chemical ratios calculated from the chemical structures

of the corresponding monomers (see Table 1). This discrepancy is due in part to additional contributions to the carbon envelopes arising from the siloxane initiator and, to a lesser extent, surface alkoxide species on the original silica sol. Indeed, the silicon signals due to the underlying silica sol are still detected, even though high degrees of polymerisation were targeted. This indicated that either the polymer overlayer was not thick enough to completely mask the underlying silica substrate or that this overlayer was 'patchy'. However, the increasing relative intensities of the various carbon components that are characteristic of the carbonyl ester groups in the methacrylic residues (i.e. the C–O–C=O and O–C=O carbon functionalities) are a clear indication of progressively higher surface concentrations of grafted polymer chains on the silica particles.

As mentioned earlier, additional sulfur and nitrogen signals were detected in the survey spectra of the silica-I-SEM(500) and silica-I-MEMA(500) composites.

For the silica-I-SEM(500) composite, the sulfur signal can be adequately peak-fitted with one component centred at 169.13 eV (spectrum not shown, see Table 4). This relatively high binding energy is characteristic of sulfate species, in good agreement with the chemical structure of the SEM monomer [34,35]. The peak-fitting of the N1s signal, observed for the silica-I-SEM(500) composite, required two sub-peaks, as shown in Fig. 5. These components are centred at 400.06 and 402.17 eV (see Table 4). These binding energies are typical of neutral amine and cationic nitrogen species, respectively [34,35]. The latter species is due to the ammonium cation of the SEM polymer. The observation of a neutral nitrogen signal is more difficult to explain. However, this signal is only about a third as intense as that due to the cationic nitrogen, and is probably best explained by surface contamination due to bipyridine ligand derived from the ATRP catalyst.

For the silica-I-MEMA(500) composite, the nitrogen signal (not shown) was peak-fitted with one component, centred on 399.54 eV, which is assigned to neutral amine species [34,35]. The detection of one nitrogen component is in good agreement with the expected neutral MEMA homopolymer structure. This observation contrasts with the silica-I-SEM composite (see above).

For all five silica-I-polymer composites, as well as the bare silica and silica-initiator reference materials, the Si2p envelope can be peak-fitted with just one component, centred at 103.6 ± 0.1 eV. This binding energy is characteristic of the underlying inorganic silica substrate, as expected. This result confirms that the decision to charge reference the carbon CC/CH signal at 285.0 eV was justified.

All the functionality assignments and binding energies of the various components for the carbon, nitrogen, sulfur and silicon species are summarised in Table 4. In addition, for the peak-fitted C1s and N1s signals, the

Table 4
Binding energies (eV) and relative peak intensities (%) of the various components of the C1s, Si2p, S2p and N1s peak-fitted signals

Sample	C1s					Si2p	S2p	N1s	
	CC/CH	C–COO C–S*	C-N	C–O	O–C=O	SiO$_2$	SO$_4^-$	N	N$^+$
SiO$_2$	285.00 eV 81.2%			286.80 eV 14.3%	288.69 eV 4.5%	103.67 eV			
SiO$_2$-Init	285.00 eV 77.1%	285.62 eV 3.0%		286.76 eV 16.9%	289.06 eV 3.1%	103.69 eV			
SiO$_2$-Init-OEGMA(250)	285.00 eV 61.5%	285.61 eV 8.9%		286.81 eV 22.0%	289.09 eV 7.6%	103.53 eV			
SiO$_2$-Init-OEGMA(500)	285.00 eV 46.4%	285.59 eV 8.9%		286.81 eV 36.9%	289.06 eV 7.8%	103.52 eV			
SiO$_2$-Init-OEGMA(1000)	285.00 eV 36.7%	285.60 eV 8.7%		286.83 eV 46.9%	289.07 eV 7.6%	103.46 eV			
SiO$_2$-Init-SEM(500)	285.00 eV 49.3%	285.75 eV 18.9%		287.00 eV 22.6%	289.15 eV 9.2%	103.61 eV	169.13 eV	400.06 eV 36.8%	402.17 eV 63.2%
SiO$_2$ -Init-MEMA(500)	285.00 eV 19.7%	285.61 eV 11.3%	286.03 eV 31.11%	286.70 eV 27.8%	289.04 eV 10.0%	103.66 eV		399.54 eV	

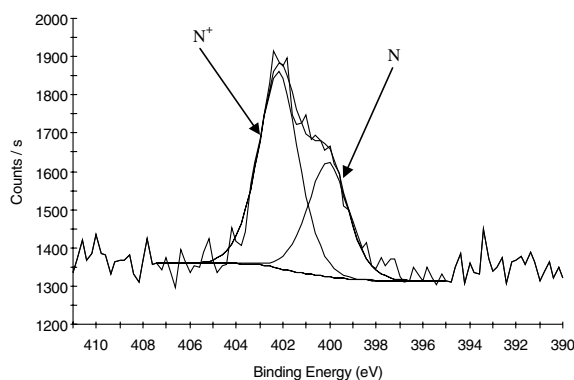*: In case of silica-init-SEM(500) composite particles only.

Fig. 5. Peak-fitted N1s signal observed for the silica-init-SEM(500) particles.

relative intensities (in %) of each component are also reported where appropriate. The binding energies determined for the various components of the C1s, N1s and S2p signals detected for the composite particles are in good agreement with the binding energies measured for solution-cast films of the corresponding pure methacrylic polymers [34,35].

Table 5 summarises the elemental surface compositions (in atom %) of the various silica-I-polymer composites and the two silica-based reference materials.

For the bare silica particles a rather high surface carbon content is observed. This is probably due to incomplete hydrolysis of alkoxide species during the Stöber synthesis, as suggested earlier on the basis of the peak-fitted C1s signal revealing the presence of oxygen-containing carbon species.

Surface modification of the silica using the bromo-functionalised siloxane initiator leads to a relative increase in the carbon content and a slight decrease in the proportion of surface silicon. It should be noted that no bromine signal was detected by XPS. This observation suggests that the surface bromine concentration is lower than the XPS detection limit. Given the chemical structure of the initiator, the C:Br:Si atomic ratio is 9:1:1 (the ethoxy groups bonded to silicon should be fully hydrolysed during grafting to the silica substrate), thus a significant increase in the carbon signal is expected for the initiator-functionalised silica compared to the bare silica sol.

The subsequent ATRP of hydrophilic methacrylates leads to a significant increase in the carbon content and a concomitant decrease in the silicon content. In the case of OEGMA monomer, higher degrees of polymerisation (D_p) were targeted by increasing the monomer concentration relative to that of the surface-grafted initiator, which led to an increase in the surface carbon concentration relative to that of silicon. This result is consistent with an increase in the polymer content with increasing target D_p, since longer chains should provide a thicker overlayer and hence gradually mask the underlying silica substrate. For the two composites prepared using the MEMA and SEM monomers, additional nitrogen signals (and also sulfur in the case of SEM) are clearly detected. In the case of silica-I-SEM, the sulfur to

Table 5
Elemental surface compositions (in atom %) for the bare silica sol, initiator-functionalised silica sol and the five polymer-grafted silica particles determined by XPS analysis

Sample	C	O	Si	N	S
SiO$_2$	18.0	56.4	25.6	–	–
SiO$_2$-init	30.4	46.7	22.9	–	–
SiO$_2$-init-OEGMA(250)	57.2	30.3	12.5	–	–
SiO$_2$-init-OEGMA(500)	57.5	32.5	10.0	–	–
SiO$_2$-init-OEGMA(1000)	59.4	32.3	8.2	–	–
SiO$_2$-init-SEM(500)	43.1	38.8	10.1	4.2	3.6
SiO$_2$-init-MEMA(500)	54.1	31.0	9.1	5.6	–

nitrogen atomic ratio is slightly less than unity; we have no satisfactory explanation for this result at the present time. The observation of these unique elemental markers clearly demonstrates the presence of the grafted polymer chains at the surface of the silica particles.

XPS characterisation of these silica-I-polymer composites clearly demonstrates significant changes in their surface compositions relative to those of the reference materials. Fig. 6 summarises the C/Si atomic ratios observed for bare silica, initiator-functionalised silica and the silica-I-polymer composites. For the initiator-functionalised silica particles, the C/Si atomic ratio increases slightly compared to the bare silica particles, due to the presence of the grafted initiator. For the silica-I-polymer composites, the C/Si atomic ratios increase by a factor of 3.2 for silica-I-SEM and by up to 5.5 for silica-I-OEGMA(1000), compared to the initiator-functionalised silica particles. These results indicate the presence of the grafted polymer chains at the silica surface. Moreover, in the case of OEGMA monomer, increasing the target degree of polymerisation led to an increase in the C/Si atomic ratio. However, it should be noted that the silica substrate is still detected, even at the highest target degree of polymerisation and regardless of the monomer structure. This observation suggests that, under the ultrahigh vacuum conditions required for XPS, the thickness of the grafted polymer overlayer is less than the expected XPS sampling depth (typically less than 10 nm for polymeric materials) [33].

Similarly, using the peak areas of the various components of the peak-fitted C1s and Si2p signals in conjunction with the appropriate elemental sensitivity factors for the XPS spectrometer, the chemical ratios for the various composites and the two reference materials can be determined. The corrected intensity ratio $I_{correct}$ is defined by the following equation:

$$I_{correct} = \frac{I_{C-O}/S_C}{I_{Si}/S_{Si}}$$

where I_{C-O} and I_{Si} represent the peak area of the carbon atoms linked via single bonds to oxygen and the peak area of the silicon components, respectively and S_C and S_{Si} are the corresponding sensitivity factors for the C1s
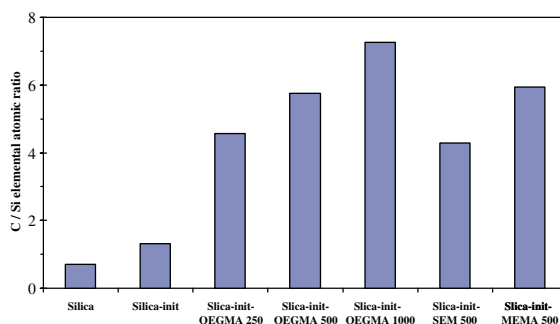

Fig. 6. XPS carbon/silicon elemental ratios obtained for bare silica sol, the initiator-functionalised silica particles, and various polymer-grafted silica particles.

and Si2p signals. The C–O component of the peak-fitted C1s signal was chosen in view of its higher relative intensity and also because it is diagnostic for polymerised methacrylic residues. Moreover, in the case of the OEGMA monomer, the pendant oligo(ethylene glycol) chains contain many C–O bonds. Thus grafting of OEGMA-based chains should lead to significant changes in the C–O component compared to the initiator-functionalised silica particles.

Fig. 7 shows the corrected intensity ratio, $I_{correct}$, determined for silica, initiator-functionalised silica and several silica-I-polymer composites. This ratio increases by a factor of up to 16.4 for the silica-I-polymer composites compared to the original initiator-functionalised silica particles. This result corroborates the increase in the C/Si atomic ratios, as previously discussed. Increasing the target D_p leads to an increase in the $I_{correct}$ ratio for the three silica-I-OEGMA composites. It is noteworthy that using the area of the carbonyl component (i.e. $I_{O-C=O}$), instead of that of the C–O component, leads to a similar trend of increasing $I_{correct}$ ratios.

The XPS characterisation of the silica–polymer composite materials demonstrates significant systematic changes in both their surface elemental and chemical compositions, compared to the initiator-functionalised silica particles. Since XPS is a very surface sensitive
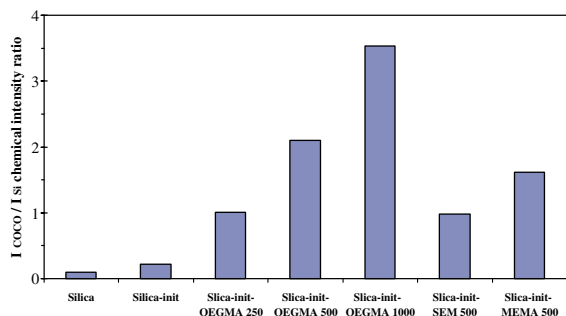
Fig. 7. Corrected $(I_{C-O}/S_C)/(I_{Si}/S_{Si})$ intensity ratios obtained from XPS studies of bare silica, initiator-functionalised silica and various polymer-grafted silica particles.

technique, the changes in composition observed clearly demonstrate that a polymeric methacrylate outerlayer is grafted onto the silica surface using the ATRP protocol. This XPS study is in good agreement with the previously reported aqueous solution properties of the silica-I-polymer composites and strongly supports their "core–shell" morphology.

4. Conclusions

This study demonstrates that initiator-functionalised silica particles can be used as a suitable colloidal substrate for the surface polymerisation of non-ionic (OEGMA), cationic (MEMA) and anionic (SEM) hydrophilic methacrylates using aqueous ATRP. XPS characterisation of the polymer grafted-silica particles indicates significant changes in their surface compositions compared to the initiator-functionalised silica sol. In addition, the detection of unique elemental markers (i.e. N1s and S2p) that are characteristic of the specific monomers, confirms the presence of thin polymeric grafted layers at the silica surface. Varying the monomer concentration relative to the surface-grafted initiator allows some control over the thickness of the grafted polymer chains. Moreover, changes in the relative intensities of the peak-fitted carbon signals of the polymer-grafted silica particles compared to the reference silica particles provide further evidence for the grafted polymer chains. This study demonstrates that efficient surface-initiated ARTP of cationic, anionic and neutral hydrophilic monomers can be performed.

References

[1] Wang JS, Matyjaszewski K. Macromolecules 1995;28: 7901.
[2] Matyjaszewski K, Xia J. Chem Rev 2001;101:2921.
[3] Robinson KL, Khan MA, de Paz Bañez MV, Wang XS, Armes SP. Macromolecules 2001;34:3155.
[4] Wang XS, Jackson SF, Armes SP. Macromolecules 2000; 33:255.
[5] Wang XS, Armes SP. Macromolecules 2000;33:6640.
[6] Wang XS, Lascelles SF, Jackson RA, Armes SP. Chem Commun 1999:1817.
[7] Ashford EJ, Naldi V, O'Dell R, Billingham NC, Armes SP. Chem Commun 1999:1285.
[8] Bütün V, Lowe AB, Billingham NC, Armes SP. J Am Chem Soc 1999;121:4288.
[9] Lobb EJ, Ma IY, Billingham NC, Armes SP. J Am Chem Soc 2001;32:7913.
[10] Liu S, Billingham NC, Armes SP. Angew Chem 2001; 40:2328.
[11] Bütün V, Armes SP, Billingham NC. Polymer 2001; 42:5993.
[12] Unali GF, Bütün V, Boucher S, Robinson KL, Billingham NC, Armes SP. Macromolecules 2001;34:6839.
[13] von Werne T, Patten TE. J Am Chem Soc 2001;123: 7497.
[14] Pyun J, Matyjaszewski K. Chem Mater 2001;13:3436.
[15] Jones DM, Huck WTS. Adv Mater 2001;13:1256.
[16] Shah RR, Merreceyes D, Husemann M, Rees I, Abbott NL, Hawker CJ, et al. Macromolecules 2000;33:597.
[17] Ejaz M, Ohno K, Tsujii Y, Fukuda T. Macromolecules 2000;33:2870.
[18] Zhao B, Brittain WJ. Macromolecules 2000;33:8813.
[19] Zhao B, Brittain WJ, Zhou W, Cheng SZD. Macromolecules 2000;33:8821.
[20] Matyjaszewski K, Miller PJ, Shukla N, Immaraporn B, Gelman A, Luokala BB, et al. Macromolecules 1999; 32:8716.
[21] Manuszak-Gerrini M, Charleux B, Vairon JP. Macromol Rapid Commun 2000;21:669.
[22] Nuß S, Böttcher H, Wurm H, Hallensleben ML. Angew Chem 2001;40:4016.
[23] Böttcher H, Hallensleben ML, Nuß S, Wurm H. Polym Bull 2000;44:223.
[24] Mandal TK, Fleming MS, Walt DR. Chem Mater 2000;12:3481.
[25] von Werne T, Patten TE. J Am Chem Soc 1999;121:7409.
[26] von Werne T, Patten TE. J Am Chem Soc 2001;123:7497.
[27] Farmer SC, Patten TE. Chem Mater 2001;13:3920.
[28] Chen X, Randall DP, Perruchot C, Watts JF, Patten TE, von Werne T, et al. J Coll Interf Sci 2003;257:56.
[29] Chen X, Armes SP. Adv Mater 2003;15:1558.
[30] Perruchot C, Khan MA, Kamitsi A, Armes SP, von Werne T, Patten TE. Langmuir 2001;17:4479.
[31] Philipse P, Vrij A. J Coll Interf Sci 1989;128:121.

[32] Socrates G, editor. Infrared characteristic group frequencies, tables and charts. 2nd ed. Chichester: John Wiley & Sons; 1994.

[33] Briggs D. Seah MP, editors. Practical surface analysis, Auger and X-ray photoelectron spectroscopy, 2nd ed., vol. 1. Chichester: Wiley; 1990.

[34] Beamson G, Briggs D, editors. High resolution XPS of organic polymers. The Scienta 300 database. Chichester: John Wiley & Sons; 1992.

[35] Vincent CB, editor. Handbook of monochromatic XPS spectra, polymers and polymers damaged by X-rays. Chichester: John Wiley & Sons; 2000.